Microsyst Technol (2009) 15:175–180
DOI 10.1007/s00542-008-0653-9

TECHNICAL PAPER

Macroscopic invisible cables

Nicola M. Pugno

Received: 29 February 2008 / Accepted: 30 May 2008 / Published online: 17 July 2008
© Springer-Verlag 2008

Abstract Spiders suggest to us that producing high strength over density ratio invisible cables could be of great importance. In this paper we show that such invisible cables could in principle be built, thanks to carbon nanotube bundles. Theoretical strength of $\sim$10 MPa, Young's modulus of $\sim$0.1 GPa and density of $\sim$0.1 Kg/m^3 are estimated. The theoretical strength over density ratio is huge, i.e. that of a single carbon nanotube; the strength of a real, thus defective, invisible cable is estimated to be $\sim$1 MPa. Finally, we demonstrate that such cables can be easily transported in their visible state (with bunched nanotubes) and that an efficient anti-bunching controllable mechanism, involving pressure of $\sim$1 Pa, can control the visible–invisible transition, and vice versa.

1 Introduction

Since their re- (see Pugno 2007a for details) discovery (Iijima 1991; Iijima and Ichihashi 1993; Bethune et al. 1993), carbon nanotubes have stimulated intense study. In particular, unique and extraordinary mechanical properties were predicted (Tans et al. 1997, 1998; Odom et al. 1998; Yakobson 1997, 1998; Lu 1997), such as an extremely high Young's modulus ($\sim$1 TPa), strength ($\sim$100 GPa) and consequently failure strain ($\sim$0.1), similar to those of graphite in-plane (Buongiorno Nardelli et al. 1998). Such properties have experimentally been confirmed by direct measurements (Yu et al. 2000a, b), developing a nanotensile testing apparatus by using two opposite atomic force microscope tips. Furthermore, the low carbon density ($\sim$1,300 Kg/m^3) suggests that carbon nanotubes have promising high strength and lightweight material applications, e.g., for innovative nano-electromechanical systems (Pugno 2004; Ke et al. 2005; Pugno et al. 2005).

In this paper we show that their mechanical properties are sufficient to realize macroscopic invisible cables. The paper is organized as follow: after this brief introduction (Sect. 1), the main idea to design an invisible large cable is described in Sect. 2, in Sect. 3 its nanotech feasibility is addressed, in Sect. 4 the role of defects is quantified, whereas in Sect. 5 the visible–invisible state transition is demonstrated to be easily controllable and reversible; then, we draw our conclusions (Sect. 6).

N. M. Pugno (✉)
Department of Structural Engineering, Politecnico di Torino,
Corso Duca degli Abruzzi 24, 10129 Turin, Italy
e-mail: nicola.pugno@polito.it

2 Invisible nanotube bundles

In this section we discuss the idea of large invisible cables (Pugno 2007b).

Consider carbon nanotubes arranged in a regular lattice with area fraction φ. The strength σ_C of the invisible cable, defined as the failure tensile force divided by the nominal area, is imposed by the equilibrium of the forces to be:

$$\sigma_C = \varphi\sigma_{\mathrm{NT}},\ \sigma \to E, \rho \tag{1}$$

where σ_{NT} denotes the strength of the single carbon nanotube. The same relation is derived for the cable Young's modulus E_C considering in Eq. 1 the substitution $\sigma \to E$ and E_{NT} as the Young's modulus of the single carbon nanotube, as imposed by the compatibility of the displacements. Similarly, the cable density ρ_C, defined as the cable weight divided by the nominal volume, is predicted according to Eq. 1 with the substitution $\sigma \to \rho$,

where ρ_{NT} would denote the carbon (nanotube) density, as can be easily derived by the mass balance. Thus, the same (failure) strain $\varepsilon_C = \sigma_C/E_C = \sigma_{NT}/E_{NT}$ and strength over density ratio $R = \sigma_C/\rho_C = \sigma_{NT}/\rho_{NT}$ is expected for the invisible cable and for the single nanotube. This ratio is huge, at least theoretically, e.g., as required in the mega-cable of the space elevator (Pugno 2007c). Thus, Eq. 1 can be used to connect the nanoscale properties of the single nanotube with the macroscopic properties of the invisible cable.

Assuming that the nanotubes are distributed in a regular lattice pattern, one can derive their separation p, from their external diameter d_+ (internal diameter $d_- \approx 0$) and area fraction φ, according to (Yao and Gao 2006):

$$p = \left(\sqrt{\varphi_{max}/\varphi} - 1\right)\frac{d_+}{2} \tag{2}$$

where φ_{max} stands for the maximum area fraction of a given lattice: $\varphi_{max} = \pi/\left(2\sqrt{3}\right),\ \pi/4,\ \pi/\left(3\sqrt{3}\right)$ respectively for triangular, square or hexagonal lattices.

On the other hand, indicating with λ the light wavelength, the condition for a nanotube to be invisible is:

$$d_+ \ll \lambda \tag{3a}$$

whereas to have a globally invisible cable, we require to not have interference between single nanotubes, i.e.:

$$p \gg \lambda \tag{3b}$$

We do not consider here the less strict limitations imposed by the sensitivity of the human eye, that can distinguish two different objects only if their angular distance is larger than $\sim 1'$. In other words, we want the cable to be intrinsically invisible.

Assuming $d_+/\lambda \approx 1/10$, $p/\lambda \approx 10$, from the previously reported nanotube theoretical strength, Young's modulus and density, we derive the following wavelength-independent invisible cable properties:

$$\sigma_C^{(theo)} \approx 10\ \text{MPa},\ E_C \approx 0.1\ \text{GPa},\ \rho_C \approx 0.1\ \text{Kg}/\text{m}^3 \tag{4}$$

Thus, with a sufficiently large spacing p, transparent and even invisible cables could in principle be realized. However, the very restrictive condition (3b), corresponding to non-interacting nanotubes, evidently implies a low nominal strength. Nevertheless, we may note that this condition is sufficient but not necessary. In fact, if Eq. 3b is not verified, e.g. for $p < \lambda$ thus for interacting nanotubes, we can treat the cable as an aerosol. In this case we can still have a globally transparent cable requiring that its effective refractive index $n_C \approx 1 + (n_{NT} - 1)\varphi$, n_{NT} is that of carbon nanotubes, be sufficiently close to the unity, i.e. $p^2 \gg {d_+}^2$, as well as that its effective absorption index $k_C \approx k_{NT}\varphi$, k_{NT} is that of carbon nanotubes, multiplied by the cable thickness T be sufficiently close to zero, i.e. $T \ll \frac{p^2}{d_+^2} k_{NT}^{-1}$. Consequently, for this case of interacting nanotubes, the nominal strength is improved but only sufficiently thin sheets would remain transparent.

3 Nanotech feasibility

Meter-long multiwalled carbon nanotube cables can already be realized (Zhang et al. 2005), suggesting that our proposal could become soon technologically feasible. For such a nanostructured macroscopic cable, a strength over density ratio of $R = \sigma_C/\rho_C \approx 120 - 144\ \text{KPa}/\left(\text{Kg}/\text{m}^3\right)$ was measured, dividing the breaking tensile force by the mass per unit length of the cable (the cross-section geometry was not of clear identification). Thus, we estimate for the single nanotube contained in such a cable $\sigma_{NT} \approx 170$ MPa ($\rho_{NT} \approx 1{,}300\ \text{Kg}/\text{m}^3$), much lower than its theoretical (Mielke et al. 2004) or measured (Yu et al. 2000b) nanoscale strength. This result was expected as a consequence of the larger probability to find critical defects in larger volumes (see Carpinteri and Pugno 2005). Thus, defects limit the range of applicability of long bundles based on nanotubes, as we are going to quantify (see Sect. 4). However, the cable strength is expected to increase with the technological advancement. The cable density was estimated to be $\rho_C \approx 1.5\ \text{Kg}/\text{m}^3$ (Zhang et al. 2005), thus resulting in a cable strength of $\sigma_C \approx 200$ KPa. Note that a densified cable with a larger value of $R = \sigma_C/\rho_C \approx 465\ \text{KPa}/\left(\text{Kg}/\text{m}^3\right)$ was also realized, suggesting the possibility of a considerable advancement for this technology in the near future. For such sheets a degree of transparency was observed, confirming that our proposal is realistic. Inverting Eq. 1 we deduce φ and from Eq. 2 we derive $p \approx 260$ nm (a square lattice is assumed), in good agreement with the scanning electron microscope (SEM) image analysis (Zhang et al. 2005). The nanotube characteristic diameter was $d_+ \approx 10$ nm (even if formation of fibrils with $d_+ \approx 50$ nm was observed in SEM). Considering the visible spectrum, $\lambda \approx 400$–600 nm, the condition (3a) was thus satisfied, in contrast to the condition (3b). Thus, the observed degree of transparency was a consequence of the limit thickness of the sheet.

Moreover, multiwalled carbon nanotubes with $d_+ \approx 50$ nm ($d_- \approx 0$ nm) spaced by $p \approx 5$ μm are expected to realize an invisible cable with the mechanical properties given in Eq. 4. For example, this would correspond to an invisible cable with a cross-section of 1 cm^2 and weight per unit length of only 10 μg/m, capable of supporting the weight of a man (1,000 N).

The nanotubes will remain parallel satisfying the condition (3b), if the cable will work under a sufficiently large tension, to avoid bunching (see Sect. 5). A later force at the middle of the cable will induce a maximum

strain $\varepsilon \approx s^{-2}$ before that all the nanotubes will be in contact, where s denotes the cable slenderness (length over cross-sectional nominal characteristic size). Since for a cable $s \gg 1$ (e.g. $>10^2$) a small strain, if compared with that at failure $\varepsilon_{\mathrm{NT}}^{(\mathrm{theo})} \approx \sigma_{\mathrm{NT}}^{(\mathrm{theo})} \Big/ E_{\mathrm{NT}} \approx 0.1$, will activate the nanotube interaction. In such a situation the cable would "appear" near to the point of application of the lateral force, i.e. where the conditions of Eq. 3b is not locally verified, the interaction; this behavior could help in visualizing the cable after having trapped a victim. A similar scenario will take place for a lateral force applied at the cable ends, that however will imply larger strains, i.e. $\varepsilon \approx s^{-1}$.

4 The role of defects

It is beyond doubt that high strength over density ratio invisible cables can be realized, following our proposal. The main question is related to the attainable strength σ_C, different from its theoretical value $\sigma_C^{(\mathrm{theo})}$ as a consequence of the unavoidable presence of defects. We discuss here the effect on the cable strength due to the presence of elliptical holes with axes a and b, perpendicular and parallel to the applied load, respectively. By applying quantized fracture mechanics (QFM, Pugno and Ruoff 2004; Pugno 2006a, b), that considers the crack growth in fracture quanta of size q, e.g. the distance between two broken chemical bonds in nanotubes ($\sim$0.25 nm for carbon), we can predict the strength reduction for a nanotube containing a given most critical elliptical hole defect. The QFM predictions for circular holes and sharp cracks are in agreement with quantum- and molecular-mechanics atomistic simulations (Mielke et al. 2004; Pugno and Ruoff 2004). We assume the defect to be small if compared to the nanotube diameter (i.e., we neglect the self-interaction between the defect tips). Thus, we have generalized the asymptotic law (for small b/a) (Pugno and Ruoff 2004), by including in the procedure the far field stress, as (Pugno 2007c):

$$\frac{\sigma_{\mathrm{NT}}(a,b)}{\sigma_{\mathrm{NT}}^{(\mathrm{theo})}} = \sqrt{\frac{1+2a/q(1+2a/b)^{-2}}{1+2a/q}} \tag{5}$$

Regarding the defect shape, for a sharp crack perpendicular to the applied load a/q = const and $b/q \to 0$, thus $\sigma_{\mathrm{NT}} \approx \frac{\sigma_{\mathrm{NT}}^{(\mathrm{theo})}}{\sqrt{1+2a/q}}$, and for $a/q \gg 1$, i.e. large cracks, $\sigma_{\mathrm{NT}} \propto a^{-1/2}$ in agreement with linear elastic fracture mechanics [that can (a) only treat sharp cracks and (b) unreasonably predicts an infinite defect-free strength, see Pugno and Ruoff 2004]; on the other hand, for a crack parallel to the applied load b/q = const and $a/q \to 0$ and thus $\sigma_{\mathrm{NT}} = \sigma_{\mathrm{NT}}^{(\mathrm{theo})}$, as it must be. In addition, regarding the defect size, for self-similar and small holes a/b = const and $a/q \to 0$ and coherently $\sigma_{\mathrm{NT}} = \sigma_{\mathrm{NT}}^{(\mathrm{theo})}$; furthermore, for self-similar and large holes a/b = const and $a/q \to \infty$ we deduce $\sigma_{\mathrm{NT}} \Big/ \sigma_{\mathrm{NT}}^{(\mathrm{theo})} \approx (1+2a/b)^{-1}$ in agreement with elasticity [that unreasonably predicts (c) a strength independent from the hole size and (d) tending to zero for cracks, see Pugno and Ruoff 2004]. Note the extreme consistency of Eq. 5, that removing all the limitations (a–d) represents the first law capable of describing in a unified manner all the size- and shape-effects for the elliptical holes, including cracks as limit case (Pugno 2007c). In other words, Eq. 5 shows that the two classical approaches of linear elastic fracture mechanics and elasticity are reasonable only for large defects; Eq. 5 unifies their results and extends its validity to small defects.

Imposing the force equilibrium for a cable composed by nanotubes in numerical fractions n_{ab} containing holes of axes a and b, we find the cable strength in the following form:

$$\frac{\sigma_C}{\sigma_C^{(\mathrm{theo})}} = \sum_{a,b} n_{ab} \frac{\sigma_{\mathrm{NT}}(a,b)}{\sigma_{\mathrm{NT}}^{(\mathrm{theo})}} \tag{6}$$

The summation is extended to all the different holes and $\sum_{a,b} n_{ab} = 1$; the numerical fraction n_{00} of nanotubes is defect-free. If all the nanotubes in the bundle contain identical holes $\sigma_C \Big/ \sigma_C^{(\mathrm{theo})} = \sigma_{\mathrm{NT}} \Big/ \sigma_{\mathrm{NT}}^{(\mathrm{theo})}$.

To have an idea of realistic defects we refer to the experiments on single walled carbon nanotube bundles (Yu et al. 2000b), and multiwalled carbon nanotubes (Yu et al. 2000a). According to Eq. 5 we can derive the corresponding size and shape of the defect compatible with each single observation, as reported in Table 1. This general table could help in the future interpretation of nanoscale tensile tests on different materials and structures: one example is given by the experiments on WS_2 nanotubes (Kaplan-Ashiri et al. 2006), that we have also treated in Table 1. Assuming for all the nanotubes in the invisible cable the "observed" most critical defect (Table 1), we would have for a defective invisible cable $\sigma_C \approx 1$ MPa (very large cracks would be even more critical). Thus, we conclude that invisible extremely lightweight cables with strength in the megapascal range could be realized, thanks to carbon nanotube technology.

5 Visible–invisible state transition

The nanotubes in the bundle will tend to bunch due to van der Waals surface attraction. The equilibrium contact width w of two identical nanotubes with diameter d_+ (do not

Table 1 $\sigma_{NT}^{(a,b)}/\sigma_{NT}^{(theo)}$ derived according to Eq. 4; in bold type we report the 13 different nanostrengths measured on single walled carbon nanotubes in bundle (Yu et al. 2000b); whereas in italic we report the 19 nanostrengths measured on multiwalled carbon nanotubes (Yu et al. 2000a), with the exception of the two smallest values of 0.11 and 0.12 (note that 0.18, 0.20, 0.24 and 0.37 was measured twice), for which we would need for example adjacent atomic vacancies ($\sim b/q = 1$) in half number $\sim a/q = 38$–45 and $\sim a/q = 32$–37, respectively

a/q	*b/q*											
	0	1	2	3	4	5	6	7	8	9	10	∞
0	1.00*	1.00*	1.00*	1.00*	1.00*	1.00*	1.00*	1.00*	1.00*	1.00*	1.00*	1.00
1	0.58	0.64	0.71	0.76	0.79	0.82*	0.84	0.86	0.87	0.88*	0.89	1.00
2	**0.45**	**0.48**	0.54	0.59	*0.63**	0.67	0.70	0.72	0.75*	0.76	0.78	1.00
3	0.38	0.40	0.44*	0.49	0.53	0.57	0.60	*0.63**	0.65	0.67	0.69*	1.00
4	**0.33**	*0.35*	0.38	0.42	0.46	0.49	**0.52**	0.55	0.58	0.60	0.62	1.00
5	0.30	0.31	*0.34*	***0.37***	0.41	0.44*	0.47	0.50*	**0.52**	0.54	0.56*	1.00
6	*0.28*	**0.29**	0.31	*0.34*	***0.37***	0.40	0.42	**0.45**	0.47	0.50*	**0.52**	1.00
7	*0.26*	0.27	**0.29**	0.31	*0.34*	0.36	*0.39*	0.41	0.44*	0.46	**0.48**	1.00
8	*0.24*	**0.25***	0.27	**0.29**	0.31	**0.33**	0.36	0.38	0.40	***0.43***	**0.45**	1.00
9	**0.23**	*0.24*	**0.25***	0.27	**0.29**	0.31	**0.33**	0.36	0.38	0.40	0.42	1.00
10	**0.22**	**0.22**	*0.24*	**0.25***	0.27	**0.29**	0.31	**0.33**	*0.35*	***0.37***	*0.39*	1.00
11	*0.21*	*0.21*	**0.22**	*0.24*	*0.26*	*0.28*	0.30	0.31	**0.33**	*0.35*	***0.37***	1.00
12	*0.20*	*0.20*	*0.21*	**0.23**	*0.24*	*0.26*	*0.28*	0.30	**0.32**	**0.33**	*0.35*	1.00
13	*0.19*	*0.20*	*0.20*	**0.22**	**0.23**	**0.25***	0.27	*0.28*	0.30	**0.32**	**0.33**	1.00
14	*0.19*	*0.19*	*0.20*	*0.21*	**0.22**	*0.24*	**0.25***	0.27	**0.29**	0.30	**0.32**	1.00
15	*0.18*	*0.18*	*0.19*	*0.20*	*0.21*	**0.23**	*0.24*	*0.26*	0.27	**0.29**	0.30	1.00
16	**0.17**	*0.18*	*0.18*	*0.19*	*0.21*	**0.22**	**0.23**	**0.25***	*0.26*	*0.28*	**0.29**	1.00
17	**0.17**	**0.17**	*0.18*	*0.19*	*0.20*	*0.21*	**0.22**	*0.24*	**0.25***	0.27	*0.28*	1.00
18	**0.16**	**0.17**	**0.17**	*0.18*	*0.19*	*0.20*	**0.22**	**0.23**	*0.24*	*0.26*	0.27	1.00
19	**0.16**	**0.16**	**0.17**	*0.18*	*0.19*	*0.20*	*0.21*	**0.22**	**0.23**	**0.25***	*0.26*	1.00
20	**0.16**	**0.16**	**0.16**	**0.17**	*0.18*	*0.19*	*0.20*	*0.21*	**0.23**	*0.24*	**0.25***	1.00
21	**0.15**	**0.15**	**0.16**	**0.17**	*0.18*	*0.19*	*0.20*	*0.21*	**0.22**	**0.23**	*0.24*	1.00
22	**0.15**	**0.15**	**0.16**	**0.16**	**0.17**	*0.18*	*0.19*	*0.20*	*0.21*	**0.22**	*0.24*	1.00
23	**0.15**	**0.15**	**0.15**	**0.16**	**0.17**	*0.18*	*0.19*	*0.20*	*0.21*	**0.22**	**0.23**	1.00
24	0.14	0.14	**0.15**	**0.15**	**0.16**	**0.17**	*0.18*	*0.19*	*0.20*	*0.21*	**0.22**	1.00
25	0.14	0.14	**0.15**	**0.15**	**0.16**	**0.17**	*0.18*	*0.19*	*0.20*	*0.21*	**0.22**	1.00
26	0.14	0.14	0.14	**0.15**	**0.15**	**0.16**	**0.17**	*0.18*	*0.19*	*0.20*	*0.21*	1.00
27	**0.13**	0.14	0.14	0.14	**0.15**	**0.16**	**0.17**	*0.18*	*0.19*	*0.20*	*0.21*	1.00
28	**0.13**	**0.13**	0.14	0.14	**0.15**	**0.16**	**0.16**	**0.17**	*0.18*	*0.19*	*0.20*	1.00
29	**0.13**	**0.13**	**0.13**	0.14	**0.15**	**0.15**	**0.16**	**0.17**	*0.18*	*0.19*	*0.20*	1.00
30	**0.13**	**0.13**	**0.13**	0.14	0.14	**0.15**	**0.16**	**0.16**	**0.17**	*0.18*	*0.19*	1.00
∞	0.00	0.00	0.00	0.00	0.00	0.00	0.00	0.00	0.00	0.00	0.00	$(1 + 2a/b)^{-1}$

The strengths measured in both data sets (Yu et al. 2000a, b) are reported in italic bold type. All the experiments refer to $\sigma_{NT}^{(theo)} = 100$ GPa ($q \sim 0.25$ nm). If all the nanotubes in the invisible cable contain identical holes, $\sigma_C/\sigma_C^{(theo)} = \sigma_{NT}/\sigma_{NT}^{(theo)}$. Atomistic simulations on circular holes ($a = b$ diagonal) and adjacent atomic vacancies (roughly corresponding to $b/q = 1$, second column) confirm the reported strength reductions (see Mielke et al. 2004; Pugno and Ruoff 2004). A similar interpretation was repored by Pugno (2007c)

This general table could help in the future interpretation of nanoscale tensile tests on different materials and structures: one new example is given by the experiments on WS_2 nanotubes recently investigated (Kaplan-Ashiri et al. 2006), corresponding to measured strengths of 16 (3 times), 15 (3 times), 14, 13, 12, 11, 10, 9, 8 (twice) 7 and 4 gigapascals, here rationalized (asterisks) assuming plausibly 16 GPa as the ideal material strength (only 15 GPa is not treated, probably corresponding as 16 GPa to the observation of the ideal strength)

subject to forces or constraints and with $d_- \approx 0$) can be determined using the well-known JKR theory of adhesion as (Hui et al. 2000; for single walled nanotubes, for which $d_- \approx 0$, a similar solution has been found by Tang et al. 2005):

$$w = 4\left(\frac{d_+^2 \gamma_S (1 - \nu_{NT})}{\pi E_{NT}}\right)^{1/3} \quad (7)$$

where ν_{NT} is the nanotube Poisson ratio and γ_S is the surface energy. Due to deformation near the contact region

of size wx, there is an accompanying stored elastic energy Φ_S in the portions of nanotubes in contact (of length x) that must satisfy the energy balance $d\Phi_S = 2\gamma_S x dw$; thus, by integration, $\Phi_S(x) = \frac{\pi E_{NT} d_+^2 x}{128(1-\nu_{NT}^2)}\left(\frac{w}{d_+}\right)^4$ (Glassmaker et al. 2004). Let us consider the mechanism shown in Fig. 1a, in which a moveable platform is introduced along the cable. The total potential energy of the system is $\Pi(x) = \Phi_S(x) + \frac{\sigma^2}{E_{NT}} AL - (F - F_f)(L - x) + \text{const}$, where σ is the resulting tension in the nanotube, having cross-sectional area A and length L; F denotes the anti-bunching force applied at the moveable platform and F_f is the friction force (gravity is here neglected but could be easily included in the energy balance). The energy balance implies $\frac{\Delta\Pi(x)}{\Delta x} = 2\gamma_S w$, where Δx is a minimum delamination advancement (Pugno and Ruoff 2004; Pugno 2006a, b; here $\frac{\Delta\Pi(x)}{\Delta x} \equiv \frac{d\Pi(x)}{dx}$), from which we deduce the simple relation $F = \frac{3}{2}\gamma_S w + F_f$, or the following nominal (referred to the platform surface area) pressure corresponding to the visible–invisible state transition:

$$\sigma_{v\to i} = \sigma_f + \frac{3}{\pi}\varphi\frac{\gamma_S w}{d_+^2} \tag{8a}$$

where σ_f is the friction stress. The invisible–visible state transition will take place when the platform is moved in the opposite direction, applying a nominal stress:

$$\sigma_{i\to v} = \sigma_f - \frac{3}{\pi}\varphi\frac{\gamma_S w}{d_+^2} \tag{8b}$$

Considering plausible values of $E_{NT} \approx 1$TPa, $\nu_{NT} \approx 0$, $d_+ \approx 50$ nm, $\gamma_S = \gamma_{vdW} \approx 0.01$ N/m (van der Waals), from Eq. 7 we estimate a contact transversal width of $w \approx 0.8$ nm; and thus taking $\sigma_f \approx 0$ and noting that $\varphi = \sigma_C^{(\text{theo})}/\sigma_{NT}^{(\text{theo})} \approx 10^{-4}$ for an invisible cable, we deduce from Eqs. 8 $\sigma_{v\to i} = |\sigma_{i\to v}| \approx 0.3$Pa. A negative value of $\sigma_{i\to v}$ suggests that this transition would be spontaneous (friction and gravity neglected) thanks to the existence of a "solid capillary effect", that could be used for building nanoelevators. Thus, the mechanism is very efficient requiring a small control pressure. Evidently the moving platform could be fixed at one of the two terminal ends (the bottom one in Fig. 1), to have a visible cable wound on a ratchet and becoming invisible when unwound by applying a cable stress $\sigma_{v\to i}$. On the other hand, when the cable is invisible it could spontaneously return to the visible state, by an instability towards the nanotube configuration reported in Fig. 1b. From the equilibrium of this configuration we can estimate the minimum value of p/L required to avoid the spontaneous invisible–visible transition (from $2\sigma A\tan\vartheta = \sigma_S \Delta x w$, see Fig. 1b):

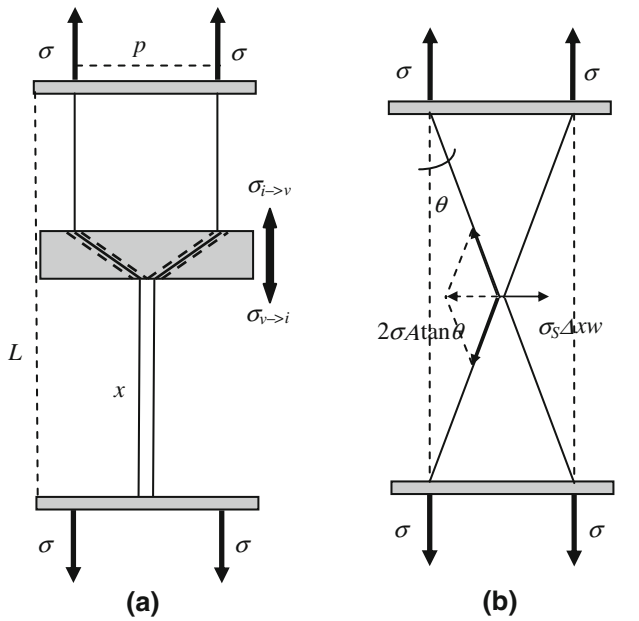

Fig. 1 Visible–invisible cable transition, and vice versa (**a**); anti-bunching condition (**b**)

$$\left.\frac{p}{L}\right|_{\min} = \frac{1}{\sqrt{1+(k\sigma/\sigma_S)^2}},\ k = \frac{\pi d_+^2}{2\Delta x w} \tag{9}$$

where σ_S is the theoretical strength of the surface interaction and σ is the applied stress in the aligned nanotubes. For example, considering $d_+ \approx 50$ nm, $\sigma_S = \sigma_{vdW} \approx 1$ MPa, $\sigma \approx 1$GPa, $\Delta x \approx w \approx 1$ nm, we deduce $p/L|_{\min} \approx 2.5 \times 10^{-7}$ ($k \approx 3927$); since for an invisible cable $p \approx 5\mu$m, $L_{\max} \approx 20$ m. Note that L here has the physical meaning of distance between two adjacent platforms and is not necessarily the total cable length: more spacer platforms along the cable can thus avoid spontaneous invisible–visible transition, even for smaller applied tension and longer cables.

6 Conclusions

Summarizing, in this paper we have shown that high strength over density ratio invisible cables could be produced in the near future, thanks to carbon nanotube technology. The cable transport will not be problematic in the visible state, whereas the visible–invisible transition can be easily controlled by the reversible and efficient proposed mechanism. Moreover, the spontaneous invisible–visible transition can be avoided by a sufficiently large cable tension and/or number of spacer platforms. Defects (in addition to the complete invisibility demand) could pose limitations to their (nominal) strength, but strongly increasable substituting the invisibility with a less

restrictive transparency demand; however their strength to density ratio is huge. Even if further detailed studies are needed, the degree of transparency observed in meter-long carbon nanotube sheets (Zhang et al. 2005) seems to confirm the validity of our idea.

Acknowledgments N.P. is supported by the ''Bando Ricerca Scientifica Piemonte 2006''—BIADS: novel biomaterials for intraoperative adjustable devices for fine tuning of prostheses shape and performance in surgery.

References

Bethune DS, Kiang CH, de Vries MS, Gorman G, Savoy R, Vazquez J, Beyers R (1993) Cobalt-catalysed growth of carbon nanotubes with single-atomic-layer walls. Nature 363:605–607

Buongiorno Nardelli M, Yakobson BI, Bernholc J (1998) Mechanism of strain release in carbon nanotubes. Phys Rev B 57:R4277–R4280

Carpinteri A, Pugno N (2005) Are the scaling laws on strength of solids related to mechanics or to geometry? Nat Mater 4:421–423

Glassmaker NJ, Jagota A, Hui CY, Kim J (2004) Design of biomimetic fibrillar interfaces: 1. Making contact. J R Soc Interface 1:23–33

Hui CY, Lin YY, Baney JM, Jagota A (2000) The accuracy of the geometric assumptions in the JKR (Johnson–Kendall–Roberts) theory of adhesion. J Adhes Sci Technol 14:1297–1319

Iijima S (1991) Helical microtubules of graphitic carbon. Nature 354:56–58

Iijima S, Ichihashi T (1993) Single-shell carbon nanotubes of 1-nm diameter. Nature 363:603–605

Kaplan-Ashiri I, Cohen SR, Gartsman K, Ivanovskaya V, Heine T, Seifert G, Wiesel I, Wagner HD, Tenne R (2006) On the mechanical behavior of WS_2 nanotubes under axial tension and compression. Proc Natl Acad Sci USA 103:523–528

Ke CH, Pugno N, Peng B, Espinosa HD (2005) Experiments and modeling of carbon nanotube NEMS devices. J Mech Phys Solids 53:1314–1333

Lu JP (1997) Elastic properties of carbon nanotubes and nanoropes. Phys Rev Lett 79:1297–1300

Mielke SL, Troya D, Zhang S, Li J-L, Xiao S, Car R, Ruoff RS, Schatz GC, Belytschko T (2004) The role of vacancy defects and holes in the fracture of carbon nanotubes. Chem Phys Lett 390:413–420

Odom TW, Huang J-L, Kim P, Lieber CM (1998) Atomic structure and electronic properties of single-walled carbon nanotubes. Nature 391:62–64

Pugno N (2004) Recent research developments in sound and vibrations. Transw Res Netw 2:197–211

Pugno N (2006a) New quantized failure criteria: application to nanotubes and nanowires. Int J Fract 141:311–323

Pugno N (2006b) Dynamic quantized fracture mechanics. Int J Fract 140:159–168

Pugno N (2007a) A journey on the nanotube, in the "Top ten advances in materials". Mater Today 11:40–45

Pugno N (2007b) Towards a Spiderman suit: large invisible cables and self-cleaning releasable super-adhesive materials. J Phys Cond Mat 19:395001 (pp 17)

Pugno N (2007c) The role of defects in the design of the space elevator cable: from nanotube to megatube. Acta Mater 55:5269–5279

Pugno N, Ruoff R (2004) Quantized fracture mechanics. Phil Mag 84:2829–2845

Pugno N, Ke CH, Espinosa H (2005) Analysis of doubly clamped nanotube devices in the finite deformation regime. J Appl Mech 72:445–449

Tang T, Jagota A, Hui CY (2005) Adhesion between single-walled carbon nanotubes. J Appl Phys 97:074304/1–6

Tans SJ, Devoret MH, Dai H, Thess A, Smalley RE, Georliga LJ, Dekker C (1997) Individual single-wall carbon nanotubes as quantum wires. Nature 386:474–477

Tans SJ, Verschueren ARM, Dekker C (1998) Room-temperature transistor based on a single carbon nanotube. Nature 393:49–52

Yakobson BI (1997) In: Ruoff RS, Kadish KM (eds) recent advances in the chemistry and physics of fullerences and related materials, electrochemical society, (Electrochemical Society, Inc., Pennington, NJ), vol 5 (97–42), p 549

Yakobson BI (1998) Mechanical relaxation, "intramolecular plasticity" in carbon nanotubes. Appl Phys Lett 72:918–920

Yao H, Gao H (2006) Mechanics of robust and releasable adhesion in biology: Bottom–up designed hierarchical structures of gecko. J Mech Phys Solids 54:1120–1146

Yu M-F, Lourie O, Dyer MJ, Moloni K, Kelly TF, Ruoff RS (2000a) Strength and breaking mechanism of multiwalled carbon nanotubes under tensile load. Science 287:637–640

Yu M-F, Files BS, Arepalli S, Ruoff RS (2000b) Tensile loading of ropes of single wall carbon nanotubes and their mechanical properties. Phys Rev Lett 84:5552–5555

Zhang M, Fang S, Zakhidov AA, Lee SB, Aliev AE, Williams CD, Atkinson KR, Baughman RH (2005) Strong, transparent, multifunctional, carbon nanotube sheets. Science 309:1215–1219